Fermi National Accelerator Laboratory

FERMILAB-Pub-84/13-E
7550.580
(Submitted to Phys. Rev. D)

BARYON PRODUCTION AND DECAY INTO STRANGE PARTICLE FINAL STATES IN 200 GeV/c π^-N INTERACTIONS

H. C. Fenker and D. R. Green
Fermi National Accelerator Laboratory, Batavia, Illinois 60510

T. Y. Chen, W. Dieterlie, E. W. Jenkins, K. W. Lai, J. LeBritton, Y. C. Lin, and A. E. Pifer
University of Arizona, Tucson, Arizona 85721

J. R. Albright, J. H. Goldman, S. L. Hagopian, J. E. Lannutti, and J. E. Piper
Florida State University, Tallahassee, Florida 32306

C. C. Chang, T. C. Davis, R. N. Diamond, K. J. Johnson, and J. A. Poirier
University of Notre Dame, Notre Dame, Indiana 46556

A. Napier and J. Schneps
Tufts University, Medford, Massachusetts 02155

J. M. Marraffino, J. W. Waters, M. S. Webster, and E. G. H. Williams
Vanderbilt University, Nashville, Tennessee 37235

J. R. Ficenec and W. P. Trower
Virginia Polytechnic Institute and State University, Blacksburg, Virginia 24061

January 1984

Baryon Production and Decay into Strange Particle Final States in 200 GeV/c π^-N Interactions

H. C. Fenker and D. R. Green
Fermi National Accelerator Laboratory*
Batavia, Illinois 60510

T. Y. Chen[a], W. Dieterlie, E. W. Jenkins, K. W. Lai,
J. LeBritton[b], Y. C. Lin[c], and A. E. Pifer
University of Arizona, Tucson, Arizona 85721

J. R. Albright, J. H. Goldman, S. L. Hagopian,
J. E. Lannutti, and J. E. Piper
Florida State University, Tallahassee, Florida 32306

C. C. Chang, T. C. Davis, R.N.Diamond[d],
K. J. Johnson[e], and J. A. Poirier
University of Notre Dame, Notre Dame, Indiana 46556

A. Napier and J. Schneps
Tufts University, Medford, Massachusetts 02155

J. M. Marraffino, J. W. Waters
M. S. Webster, and E. G. H. Williams
Vanderbilt University, Nashville, Tennessee 37235

J. R. Ficenec and W. P. Trower
Virginia Tech, Blacksburg, Virginia 24061

ABSTRACT

Baryon production and subsequent decay into $K^\circ_S\Lambda^\circ$, $\Lambda^\circ\pi^\pm$, $K^\circ_S\Lambda^\circ\pi^\pm$, and $\Lambda^\circ\pi^+\pi^-$ final states are studied. Evidence for the states N(1710), Σ(1385), Σ(1620), Σ(1690), Σ(2250), Ξ(1320), Ξ(1530), Ξ(1820), and Ξ(1940) is presented. Ratios of x_F distributions and cross sections are compared to the predictions of phenomenological models.

It has been observed that resonance production is a source of a substantial fraction of all final state stable hadrons[1]. Presumably the production characteristics of these resonances form a more direct probe of the underlying production dynamics than do those of the final state particles. In particular, the ratios of cross sections for resonances with different strangeness should probe local compensation of quantum number[2]. The ratios of x_f distributions provide tests of dimensional counting rules[3].

The experiment and data analysis procedure have been described elsewhere[4]. The data consist of ~60,000 events of the type $\pi^- N \to V^\circ V^\circ X$ where $V^\circ = K_S$, Λ°, or $\bar{\Lambda}^\circ$, and the charged multiplicity of the X state is required to be ≤ 5 for the region $x_f \geq 0.2$, where the acceptance of the apparatus was large. The mass resolution of the K_S is ± 5 MeV/c^2 for a typical momentum, $\langle P_{K_S} \rangle \sim 40$ GeV/c. Constrained fits were made to the decay vertex (1-C), V° mass (1-C), and V°-V° primary vertex (1-C). Fits are accepted if the χ^2 probability is $> 10^{-5}$. The V° identification was done by attempting K_S, Λ°, and $\bar{\Lambda}^\circ$ hypotheses and assigning the best fit hypothesis. A 5% contamination of $K_S K_S$ is estimated to exist in the $K_S \Lambda^\circ$, $K_S \bar{\Lambda}^\circ$ sample (~18,000 events) reported here.

Tracks within the spectrometer are placed into two categories. Tracks passing within $\pm 3\sigma$ of the production target are defined to be "direct" tracks. Those outside this cut are defined to be "decay" tracks. No mass identification of these secondary tracks has been attempted.

The x_f and p_t distributions for K_S, Λ°, $\bar{\Lambda}^\circ$, $K_S \Lambda^\circ$, and $K_S \bar{\Lambda}^\circ$ are consistent with those found from unbiased data[5] after corrections for acceptance are made. A check on the mass scale of this experiment is

that the unconstrained K_s and Λ° masses agree with accepted values[6] within ± 1 MeV/c^2. As a further check we examine the $K_s\pi^\pm$ mass distributions and compare the observed K*(890) and K*(1420) masses and widths to those expected given our mass resolution. The agreement is excellent.

In Figure 1 is shown the $K_s\Lambda^\circ$ plus $K_s\bar{\Lambda}^\circ$ effective mass distribution. This distribution and all subsequent mass distributions are fit with Breit-Wigner shapes for the resonances, and a background of the form

$$\{a(M-M_t) + b(M-M_t)^2 + c(M-M_t)^3\}\cdot e^{-d(M-M_t)},$$

where M_t is the threshold mass. In performing the fits, the chi-square contribution of each bin in a histogram is based on the difference between the number of events in that bin and the integral over the bin of the background plus resonance function. Masses and widths of known resonances[6] are fixed in the fits unless otherwise noted. When masses and widths are not well determined[6] the fixed values used in the fits are quoted in the text. The experimental resolution as determined from observed widths of K_s° and Λ is added in quadrature in all fits. In some cases it is necessary to exclude certain bins from the fits: either because of the inadequacy of the polynomial-exponential model in the region of sharply rising phase space, or because of understood problems with the track finding procedure. In all figures, excluded bins are indicated by shading.

The curve of Fig. 1 is such a fit with the resonances N(1710), Γ= 120 MeV/c^2, Ξ(1823), Γ= 20 MeV/c^2, and Ξ(1940), Γ= 100 MeV/c^2. The χ^2 per degree of freedom (DOF) is 110/90. If the Ξ(1940), the resonance for which the evidence is poorest (196 ±156 events), is not included in the fit, the χ^2 becomes 112 for 91 degrees of freedom. The evidence for the presence of the other two resonances is more compelling: 1422 ±356 events for the N(1710), and 142 ±68 for the Ξ(1823).

In Figure 2 the effective mass of a Λ° or $\bar{\Lambda}^\circ$ and other single spectrometer tracks is shown. In Fig. 2a the track is a "decay" track, assumed to be a pion. Only the combinations $\Lambda^\circ\pi^-$ and $\bar{\Lambda}^\circ\pi^+$ are used. A clear Ξ(1321) is seen, consisting of 350 ±35 entries, with a width (4.3 ±0.7 Mev/c^2) consistent with the mass resolution. The χ^2/DOF for this fit is 79/85. To check the accuracy of the mass scale, the fit was recalculated with the central mass allowed to vary. The result, 1321.4 ± 0.3 MeV/c^2, is in excellent agreement with the world average[6] of 1321.3 ±0.13 MeV/c^2.

The Λ° or $\bar{\Lambda}^\circ$ plus "direct" track (assumed to be a pion) effective mass is shown in Figure 2b. In this case both $\Lambda^\circ\pi^\pm$ and $\bar{\Lambda}^\circ\pi^\pm$ charge combinations are used. A very clear Σ(1385) signal is observed (428 ±110 entries) together with some Ξ(1320) signal from real decay tracks that were misidentified as direct tracks because of their forward decay topologies. The very low masses are excluded from the fit, as discussed above.

Slightly weaker evidence for the presence of Σ(1620) (M=1613, Γ=35 MeV/c^2) and Σ(1690) (M=1690, Γ=40 MeV/c^2) is also present in the data. With these resonances included in the fit, the χ^2/DOF is 62/45. Without them the best fit has χ^2/DOF = 96/47. The best fit occurs for 384 ±86

$\Sigma(1620)$ events and 352 $\pm$85 $\Sigma(1690)$ events.

In Figure 3 is shown the $\Xi^-\pi^+$ plus $\bar{\Xi}^+\pi^-$ mass distribution, where in this case and in what follows a Ξ^- is defined to be a $\Lambda^\circ\pi^-$ effective mass between 1318 MeV/c^2 and 1325 MeV/c^2. A clear $\Xi(1530)$ signal is seen with 43 $\pm$8 entries. The χ^2/DOF for the resonance plus background fit is 43/62 with the mass and width of the $\Xi(1530)$ fixed at the fitted values 1540 and 9.1 MeV/c^2, respectively.

The $K_S^\circ\Xi^-$ or $K_S^\circ\bar{\Xi}^+$ effective mass distribution is shown in Figure 4. A 2.5σ indication of $\Sigma(2250)$, 21 $\pm$8 entries, is observed with fitted central mass 2236$\pm$6 and width 7^{+13}_{-7} MeV/c^2, both of which are consistent with the wide range of values previously reported[6]. The χ^2 for the overall fit is 69 for 67 degrees of freedom.

If the production dynamics of the resonances which are observed is such that baryons and antibaryons materialize out of the quark sea in the x_f region far from the region of target fragmentation, then one expects that the baryon to antibaryon ratio will be 1. Using our data alone this ratio can be studied with very little systematic bias for baryons of different strangeness.

In order to study this question we have subdivided the data in figures 1 and 2 into different charge and baryon number states and performed fits similar to those described above. Only results for the most significant states are quoted.

For the $K_S^\circ\Lambda^\circ$ and $K_S^\circ\bar{\Lambda}^\circ$ data the resulting ratios are $\bar{N}(1710)/N(1710)$ = 1.7 $\pm$0.6 and $\bar{\Xi}^\circ(1823)/\Xi^\circ(1823)$ = 2.1 $\pm$1.9. The subdivided data of Fig. 2a yield the fitted ratio $\bar{\Xi}^+(1321)/\Xi^-(1321)$ = 0.4 $\pm$0.1. Finally, the subdivided data of Fig. 2b yield the fitted ratio $\bar{\Sigma}^\pm(1385)/\Sigma^\pm(1385)$= 0.6 $\pm$0.4.

Hence, the data appear to support crudely such a picture of resonance production, since the ratios are all consistent with 1 within the statistical accuracy except for the $\Xi(1321)$. Note that the apparatus has good detection efficiency for x_f of the $\Lambda^\circ \gtrsim 0.2$ with reduced efficiency in the region $0.0 \lesssim x_f \lesssim 0.2$, so that the data shown herein is in the pion fragmentation and central regions of production.

In order to probe the compensation of strangeness, one may examine ratios of resonances of different strangeness but with the same final state. This procedure results in a reduced systematic bias. In this case the full data of Figures 1 and 2 are used. In the $K_S^\circ\Lambda^\circ$ and $K_S^\circ\bar{\Lambda}^\circ$ final states the observed ratio, correcting for decay branching ratios, is $\{N(1710)+\bar{N}(1710)\}/\{\Xi^\circ(1823)+\bar{\Xi}^\circ(1823)\} = 45 \pm 33$. Using the $\Lambda^\circ\pi^\pm$ and $\bar{\Lambda}^\circ\pi^\pm$ data of Fig. 2a, and correcting for Ξ appearing in Fig. 2b and for decay branching ratios, one finds the ratio $\{\Xi^-(1321)+\bar{\Xi}^+(1321)\}/\{\Sigma^\pm(1385)+\bar{\Sigma}^\pm(1385)\} = 1.0 \pm 0.3$. Variations of the geometric efficiency with mass, as determined by Monte Carlo methods, are considerably less than the statistical errors on these ratios.

One may compare these cross section ratios to a phenomenological model[2]. This model has recently been successfully applied to strange particle meson resonance production at the ISR[7]. The cross section for production of a mass m is given by

$$\sigma(m) = A \cdot y_{max}^2 \cdot e^{-\alpha/y_{max}^\beta} \cdot M/(M+M_o)^\gamma \qquad (1)$$

with $\alpha = 5.13$, $\beta = 0.38$, $\gamma = 12.3$, and $M_o = 2$ GeV/c^2. In this model, M is the mass of the simplest "composite" particle consistent with the production of m and local conservation of quantum numbers. The term y_{max} is the

maximum rapidity that the composite particle is allowed to have by kinematics when it recoils off of another particle in the center of mass. In the calculations below we used a pion, but the results are not sensitive to this choice.

Given local compensation of strangeness, S, we have assumed values of M as follows: M=1710, M=1385+m_K, M=1321+2m_K, and M=1823+2m_K for the N(1710), Σ(1385), Ξ(1321), and Ξ(1823), respectively. The predicted ratios are $\{N(1710)+\bar{N}(1710)\}/\{\Xi^o(1823)+\bar{\Xi}^o(1823)\}$ = 34, and $\{\Xi^-(1321)+\bar{\Xi}^+(1321)\}/\{\Sigma^\pm(1385)+\bar{\Sigma}^\pm(1385)\}$ = 0.24, which are in rough agreement with the data.

For further discussion of our observations and comparison to other data, it is necessary to determine our cross section normalization. We take the $K_S^o\bar{\Lambda}^o$ production cross section measured in a hydrogen bubble chamber exposure[5] to 250 GeV/c π^-, and note that both the K_S^o and $\bar{\Lambda}^o$ observed in that experiment appear to be produced centrally. Thus the production mechanism observed in the present experiment (see below) appears to be the same as the one providing the calibration point. We scale their measured cross section by $(\ln s)^2$ to account for the different beam momenta and determine that our sensitivity for raw numbers of events is 68 $\pm$ 31 events per microbarn.

Table I contains the observed states, the decay modes examined, composite masses, fitted numbers of events, branching ratios, and cross sections. The N(1710) and Ξ(1820) cross sections are directly normalized to unbiased data as noted above. The errors quoted on the cross sections reflect statistical errors and those on the $K_S^o\Lambda^o$ branching ratios. There is also an overall ~50% normalization uncertainty. For the Σ(1385), Ξ(1321), and Ξ(1530) an additional set of assumptions is needed. The

geometric efficiency correction for the pions is determined from the observed decay angular distributions. It is assumed that from the observed final state, e.g. $\Lambda^{\circ}K_S^{\circ}\pi^-$, one can extract the cross section for the state $\Lambda^{\circ}\pi^-$ by multiplying by four: 2 for $\{(K_S^{\circ}+K_L^{\circ})/K_S^{\circ}\}$ and 2 for $\{(K^{\circ}+K^+)/K^{\circ}\}$. No error has been assigned to this procedure. The quoted errors reflect only statistical errors and errors on branching ratios, added in quadrature.

Other data on inclusive baryon resonance production in high energy πN interactions are rather limited. In 147 GeV/c π^+p interactions, inclusive $\Sigma^{*+}(1385)$ was observed[8] with a cross section of 290±70 μb, and an upper limit was set on $\Sigma^{*-}(1385)$ production of 100 μb. At the ISR, $\Sigma^{*\pm}(1385)$ and $\Xi^-(1320)$ were observed[9] for $x_f > 0.4$ with cross sections 250 μb, 40 μb, and 9 μb for Σ^{*+}, Σ^{*-}, and Ξ^- respectively. In 240 GeV/c pp interactions at $x_f = 0.48$, $P_t = 600$ MeV/c the production of Ξ^-, $\bar{\Xi}^+$, Ω^-, and $\bar{\Omega}^+$ has been observed[10]. The latter two experiments have studied the proton fragmentation region, while this experiment observes the entire forward hemisphere consisting of the central and π^- fragmentation regions. Other data on baryon resonance production have been compiled[1,11] and are used for comparison.

Figure 5 shows the relationship among our measured cross sections, the model[2], and the other data [1,10,11] extrapolated to our center of mass energy using the model of reference 2. The curve shows the cross section prediction of the model as a function of the "composite" particle mass M, where this mass is given in Table I. The factor A in equation (1) is taken to have the value 0.4×10^{-20} cm^{-2} which was used successfully in ref. 10 to predict mesonic resonance cross sections in pp collisions at ISR energies. For the other data on ρ, K*(890), K*(1420), f', g, and A

we have taken "composite" masses M of 770, $890+m_K$, $1420+m_K$, 1515, 1690, and $1115+m_K$, respectively. Clearly the main trends of the data are consistent with this model, given our choice of M for meson and baryon states. This model incorporates central production of resonances and local conservation of strangeness and baryon number. The present data set extends the range of data in M and $\sigma(m)$ substantially.

Other information concerning production dynamics may be obtained from the x_f distributions. In Fig 6 is shown the ratio of $\bar{\Lambda}^\circ$ and Λ° differential cross sections $d\sigma/dx_f$ as a function of x_f. The curve is a best fit[12] to analogous data on $\pi^- p \to \bar{p}X$ and $\pi^- p \to pX$ whose general behavior agrees with the present data. At $x_f \sim 0$ the $\bar{\Lambda}^\circ/\Lambda^\circ$ ratio is ~0.5, perhaps indicating some contamination due to proton fragmentation. For $0.1 \lesssim x_f \lesssim 0.6$ one has $\bar{\Lambda}^\circ/\Lambda^\circ \sim 0.75$. In the region $x_f \gtrsim 0.6$ the $\bar{\Lambda}^\circ/\Lambda^\circ$ ratio increases, indicating that the $\bar{u}$ valence quark (shared with the $\bar{\Lambda}^\circ$) in the π^- dominates over the d valence quark (shared with the Λ°).

In Figures 7a and 7b are shown the x_f distributions of the $\Sigma^{\pm}(1385)$ + $\bar{\Sigma}^{\pm}(1385)$ and $\Xi^-(1321)$ + $\bar{\Xi}^+(1321)$, after correction for experimental acceptance has been applied and background has been subtracted. The curves are fits to $(1/\sigma)d\sigma/dx = \alpha(1-x)^n$, where n for the $\Sigma(1385)$ is 5.8 ± 1.7 and for the $\Xi(1321)$ is 6.7 ± 0.3. Although the available statistics do not allow any definitive statement about the relative shapes of these distributions, it can be seen that both of these states are produced in the central kinematic region, and that the exponents, n, are consistent with dimensional counting schemes[3]. There is a trend for the $\Xi(1321)$ to be produced more centrally than the $\Sigma(1385)$. One might expect this trend due to the fact that two strange quarks need to be

extracted from the sea to produce a Ξ while only one is needed to make a Σ.

In conclusion we have observed baryons with strangeness 0,1, and 2 in $\pi^- N$ interactions. Their production cross section ratios are consistent with a central production mechanism with local quantum number compensation. Their x_f distributions are consistent with analogous data and also provide evidence of central production.

ACKNOWLEDGEMENTS

We thank the Fermilab staff, especially S. Hansen and R. Cantal, for their valuable help during this experiment. Z. Ma provided helpful support. The work was supported in part by Department of Energy contracts (Arizona, Florida State, Tufts) and National Science Foundation grants (Arizona, Notre Dame, Vanderbilt and Virginia Tech.).

FOOTNOTES

*) Operated by Universities Research Association Inc. under Contract with the United States Department of Energy.

a) Permanent address: Dept. of Physics, Nanking U., Nanking, CHINA.

b) Present address: Burr Brown Research Corp., 6730 S. Tucson Blvd., Tucson, Arizona 85706

c) Present address: High Energy Physics Lab., Stanford U., Stanford, California 94305

d) Former address: Florida State U., Tallahassee, Florida 32306

e) Present address: Motorola Inc., P.O. Box 2953, Phoenix, Arizona 85062

REFERENCES

1. J. Whitmore, Proceedings of the XIX International Conference on High Energy Physics, Ed. S. Homma, M. Kawaguchi, H. Miyazawa, Tokyo, 1978, p. 63.
2. M. Bourguin, J. M. Gaillard, Nuc. Phys. B114, 334 (1976).
3. R. Blankenbecker, S. J. Brodsky, Phys. Rev. D10, 2973 (1974) and S. J. Brodsky, J. F. Gunion, Phys. Rev. D17, 848 (1978).
4. T. Y. Chen et al., Phys. Rev. D28, 2304 (1983).
5. D. Bogert et al., Phys. Rev. D16, 2098 (1977).
6. M. Ross et al., Phys. Lett. 111B, 1 (1982).
7. A. Bohm et al., Phys. Rev. Lett. 41, 1761 (1978).
8. D. Brick et al., Phys. Rev. D25, 2248 (1982).
9. S. Erhan et al., Phys. Lett. 85B, 447 (1979).
10. M. Bourguin et al., Z. Physik C5, 275 (1980).
11. S. Hagopian et al., Private Communication (1977).
12. D. Cutts et al., Phys. Rev. Lett. 43, 319 (1979).

TABLE CAPTIONS

Table I. The parameters of the baryon states for this experiment which are plotted in Fig. 5.

STATE (MeV)	DECAY MODE	COMPOSITE MASS (MeV)	EVENTS	BR (%)	σ (μb)
N(1710)	$K_S^0\Lambda^0$ or $K_S^0\bar{\Lambda}_0$	1710	1422±356	10±5	418±200
Σ(1385)	$\Lambda^0\pi^\pm$ or $\bar{\Lambda}^0\pi^\pm$	1879	428±110	88±2	23±8
Σ(1620)	$\Lambda^0\pi^\pm$ or $\bar{\Lambda}^0\pi^\pm$	2114	334±86	--	--
Σ(1690)	$\Lambda^0\pi^\pm$ or $\bar{\Lambda}^0\pi^\pm$	2184	352±85	--	--
Σ(2250)	$K_S^0\Xi^-$ or $K_S^0\bar{\Xi}^+$	2744	21±8	--	--
Ξ(1320)	$\Lambda^0\pi^-$ or $\bar{\Lambda}^0\pi^-$	2308	350±35	100	41±4
Ξ(1530)	$\Xi^-\pi^+$ or $\bar{\Xi}^+\pi^-$	2518	43±8	100	11±2
Ξ(1820)	$K_S^0\Lambda^0$ or $K_S^0\bar{\Lambda}^0$	2808	142±68	45±10	9.4±4.4
Ξ(1940)	$K_S^0\Lambda^0$ or $K_S^0\bar{\Lambda}^0$	2928	196±156	--	--

FIGURE CAPTIONS

Fig. 1. Effective mass of the $K^0_S\Lambda^0$ or $K^0_S\bar{\Lambda}^0$ events. The dashed curves are fitted to background and resonances as described in the text; the solid curve is the sum of all the contributions. The shaded portion is excluded from the fit.

Fig. 2a. Effective mass of the $\Lambda^0\pi^-$ or $\bar{\Lambda}^0\pi^+$ entries for those pions which miss the primary interaction point by more than 3 sigma. The dashed curves are fitted to background and resonance as described in the text; the solid curve is the sum of all the contributions. The shaded portion is excluded from the fit.

Fig. 2b. Effective mass of the $\Lambda^0\pi^-$, $\Lambda^0\pi^+$, $\bar{\Lambda}^0\pi^-$ or $\bar{\Lambda}^0\pi^+$ entries for those pions which are within 3 sigma of the interaction point. The dashed curves are fitted to background and resonances as described in the text; the solid curve is the sum of all the contributions. The shaded portion is excluded from the fit.

Fig. 3. Effective mass of the $\Xi^-\pi^+$ $\bar{\Xi}^+\pi^-$ entries. The dashed curves are fitted to background and resonance as described in the text; the solid curve is the sum of all the contributions.

Fig. 4. Effective mass of the $\Xi^- K^0_S$ or $\bar{\Xi}^+ K^0_S$ entries. The dashed curves are fitted to background and resonance as described in the text; the solid curve is the sum of all the contributions.

Fig. 5. Inclusive cross section for the production of mesons and baryons at 200 GeV/c laboratory momentum as a function of the composite mass, M, as defined in the text. The data is from the present experiment as well as references Whitmore[1], ISR[10], and FSU[11]. The error bars for this experiment do not include systematic uncertainties in our cross section normalization. The curve is a calculation using the model in Reference 2.

Fig. 6. The ratio of the $\bar{\Lambda}^0$ to Λ^0 differential cross sections $d\sigma/dx$ plotted as a function of Feynman x. The curve is a fit to the $\bar{p}$ to p ratio from Reference 12.

Fig. 7. The Feynman x distributions of $(1/\sigma)d\sigma/dx$ for a) $\Sigma(1385)$ and b) $\Xi(1321)$. The curves are best fits to the form $(1/\sigma)d\sigma/dx = \alpha(1-x)^n$.

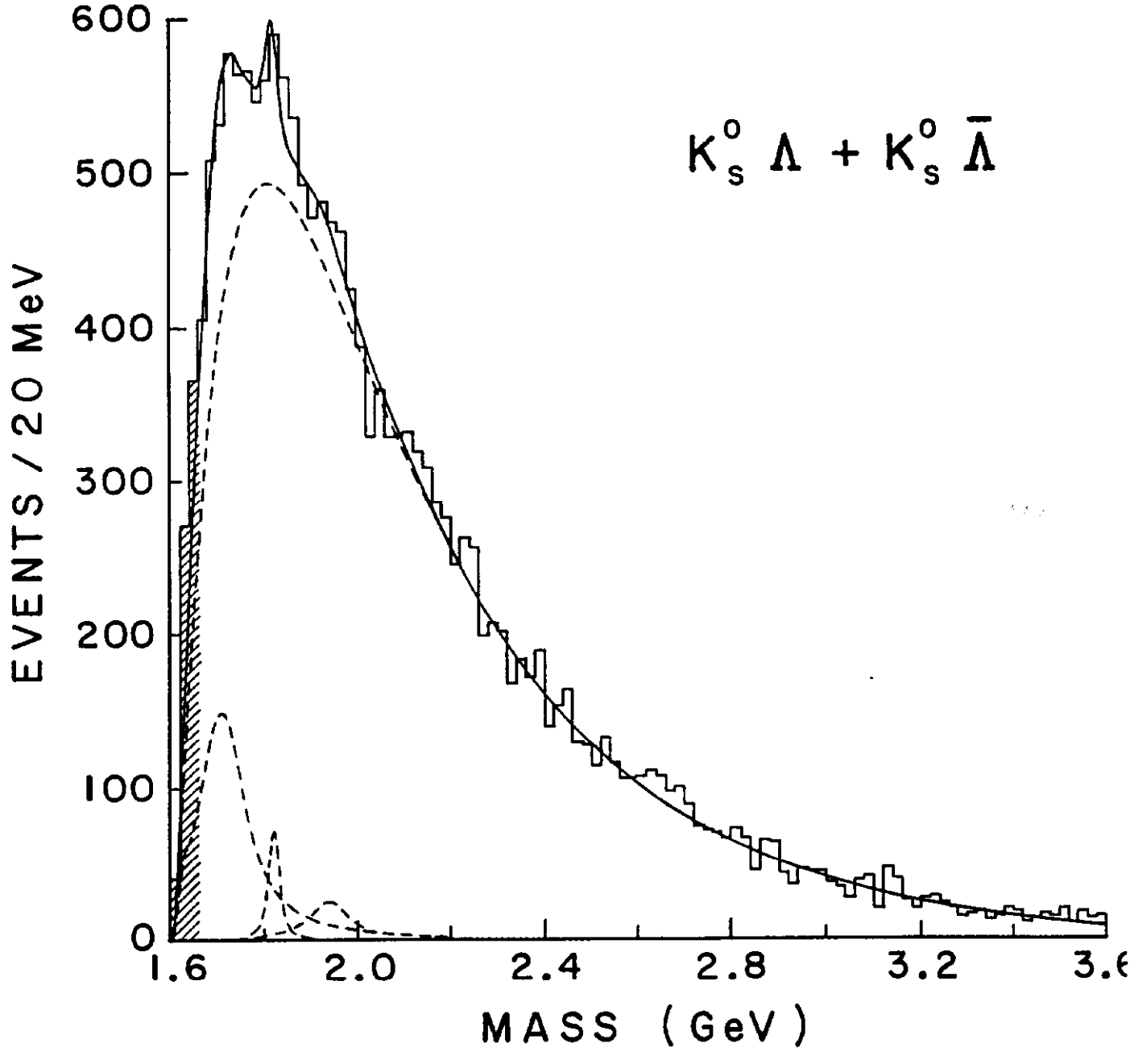
600
500
400
300
200
100
0
EVENTS / 20 MeV
1.6
2.0
2.4
2.8
3.2
MASS (GeV)
$K^0_s \Lambda + K^0_s \bar{\Lambda}$

Figure 1

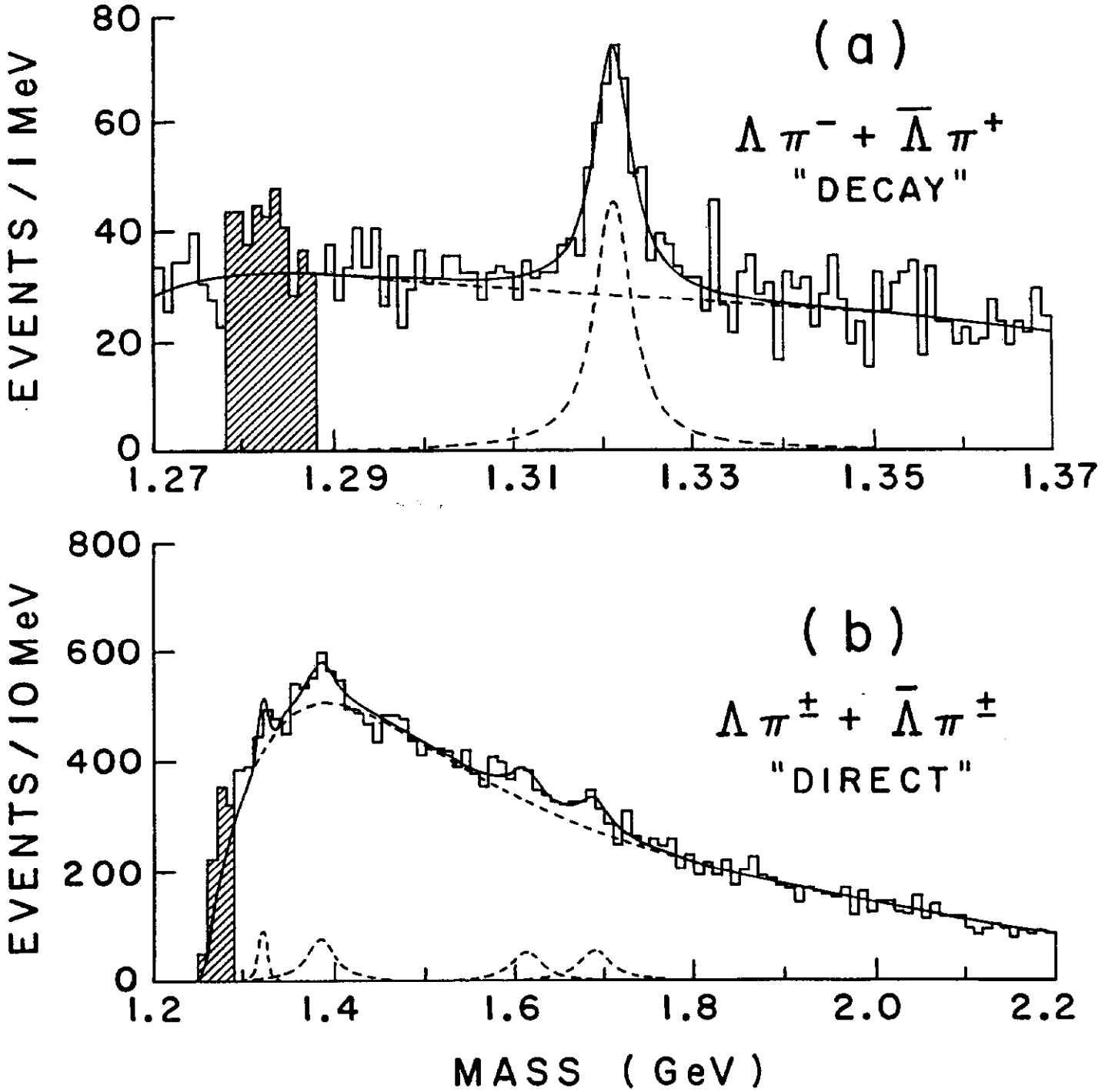
(a)
$\Lambda\pi^- + \bar{\Lambda}\pi^+$
"DECAY"
EVENTS / 1 MeV
80
60
40
20
0
1.27
1.29
1.31
1.33
1.35
1.37
(b)
$\Lambda\pi^\pm + \bar{\Lambda}\pi^\pm$
"DIRECT"
EVENTS / 10 MeV
800
600
400
200
0
1.2
1.4
1.6
1.8
2.0
2.2
MASS (GeV)

Figure 2

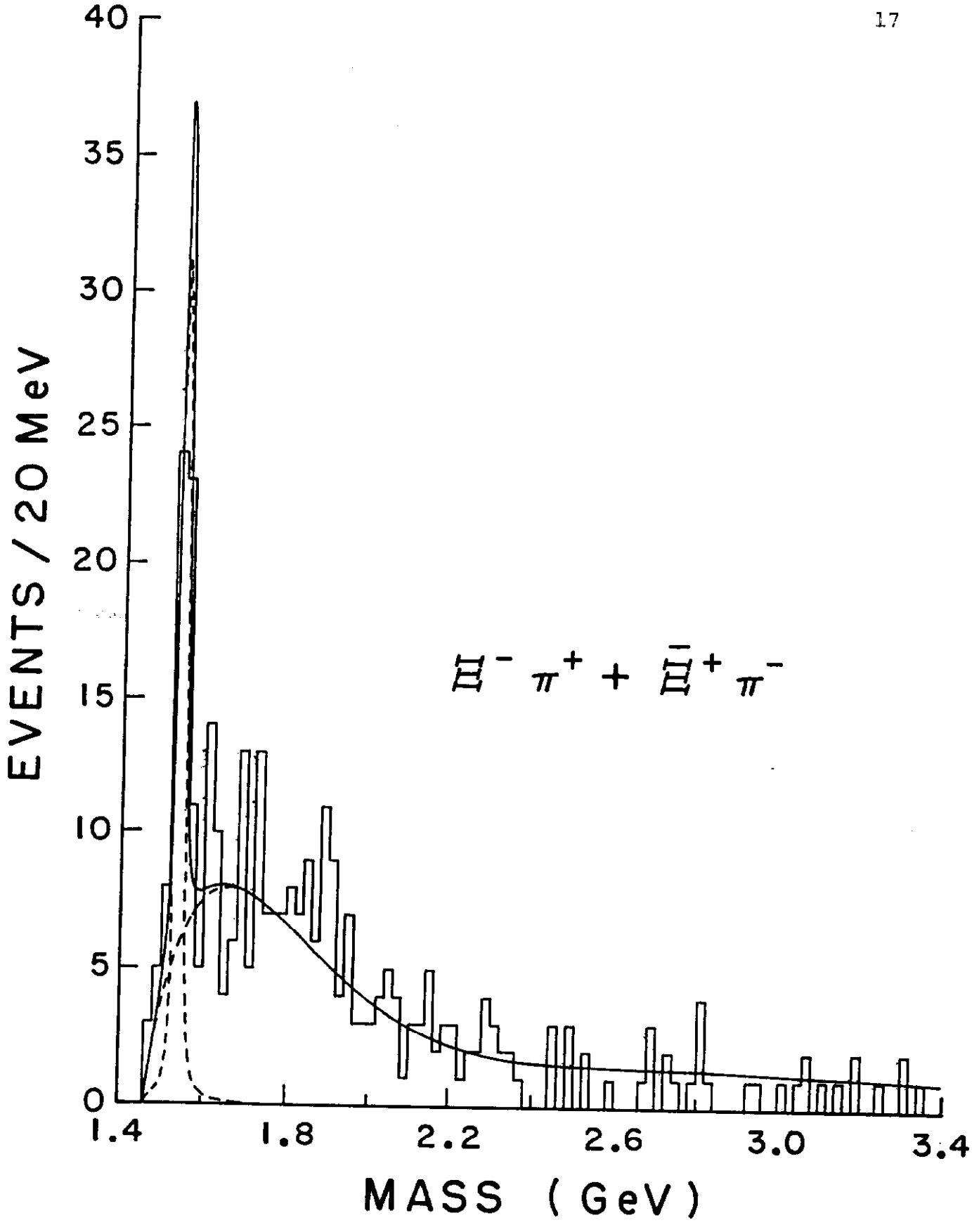
EVENTS / 20 MeV
40
35
30
25
20
15
10
5
0
1.4
1.8
2.2
2.6
3.0
3.4
MASS (GeV)
$\Xi^- \pi^+ + \bar{\Xi}^+ \pi^-$

Figure 3

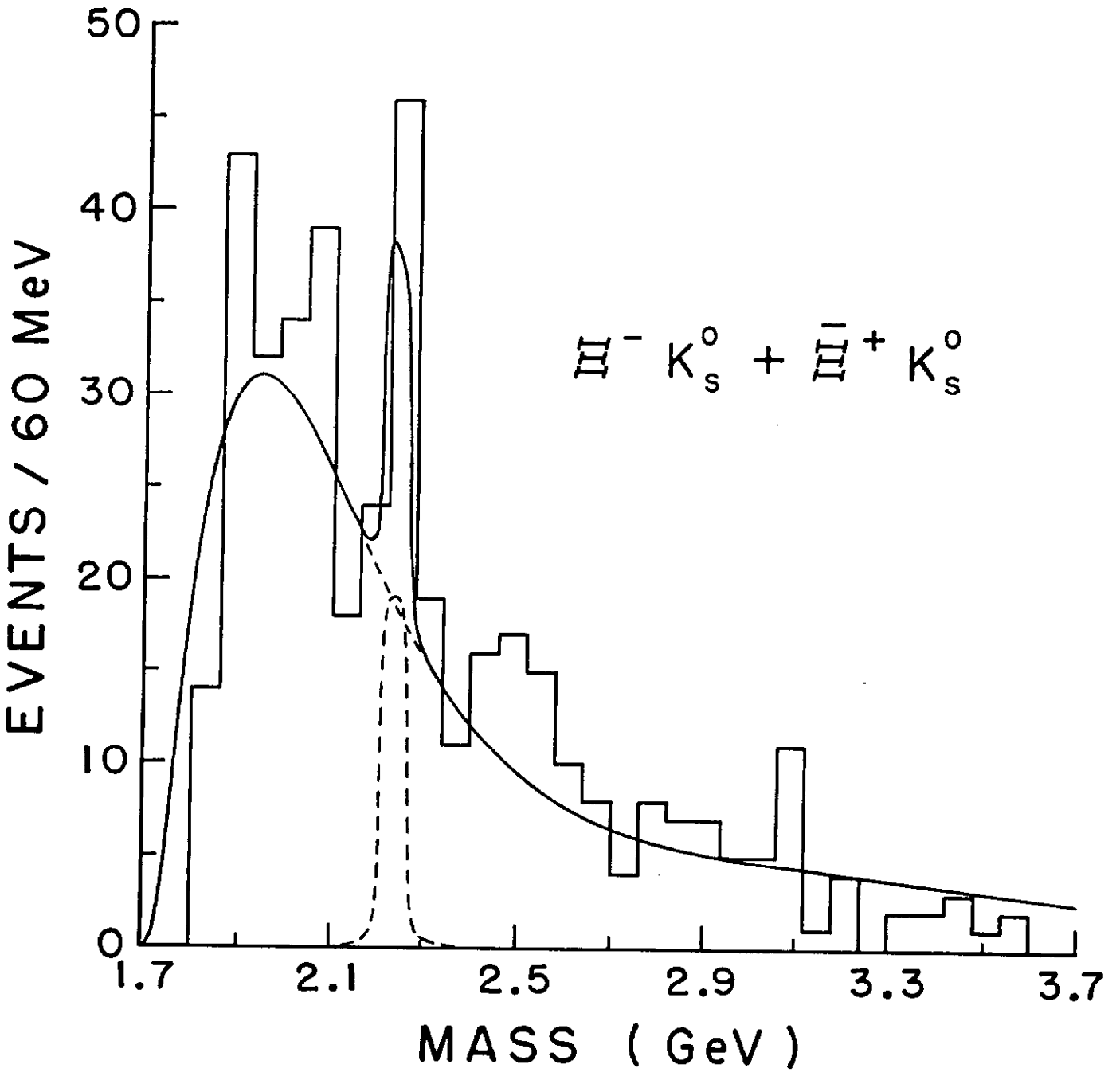
50
40
30
20
10
0
EVENTS / 60 MeV
$\Xi^- K_s^0 + \bar{\Xi}^+ K_s^0$
1.7
2.1
2.5
2.9
3.3
3.7
MASS (GeV)

Figure 4

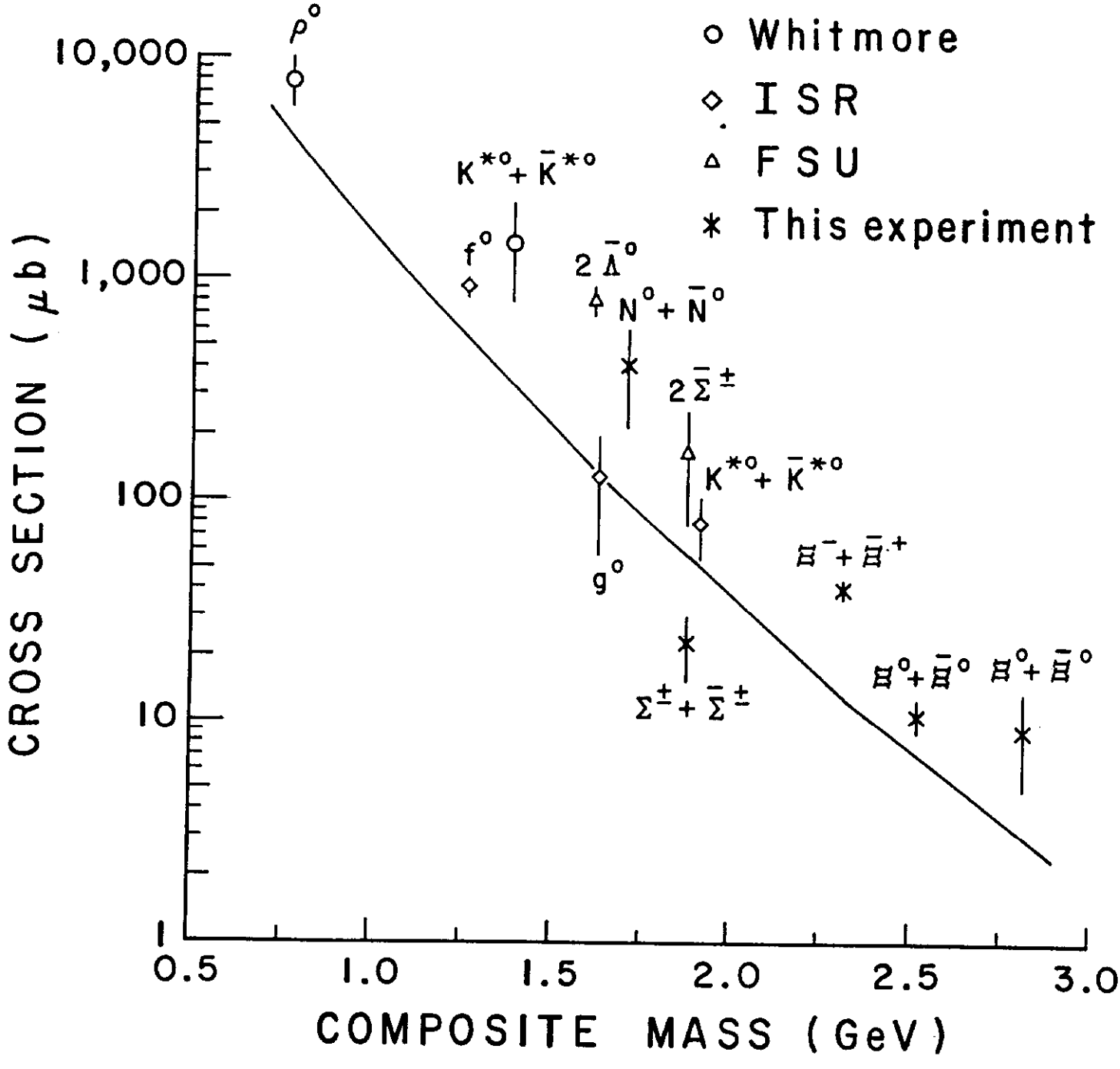
CROSS SECTION (μb)
10,000
1,000
100
10
1
0.5
1.0
1.5
2.0
2.5
3.0
COMPOSITE MASS (GeV)
ρ°
K*° + K̄*°
f°
2 Λ̄°
N° + N̄°
2 Σ̄±
K*° + K̄*°
g°
Ξ⁻ + Ξ̄⁺
Σ± + Σ̄±
Ξ° + Ξ̄°
Ξ° + Ξ̄°
Whitmore
ISR
FSU
This experiment

Figure

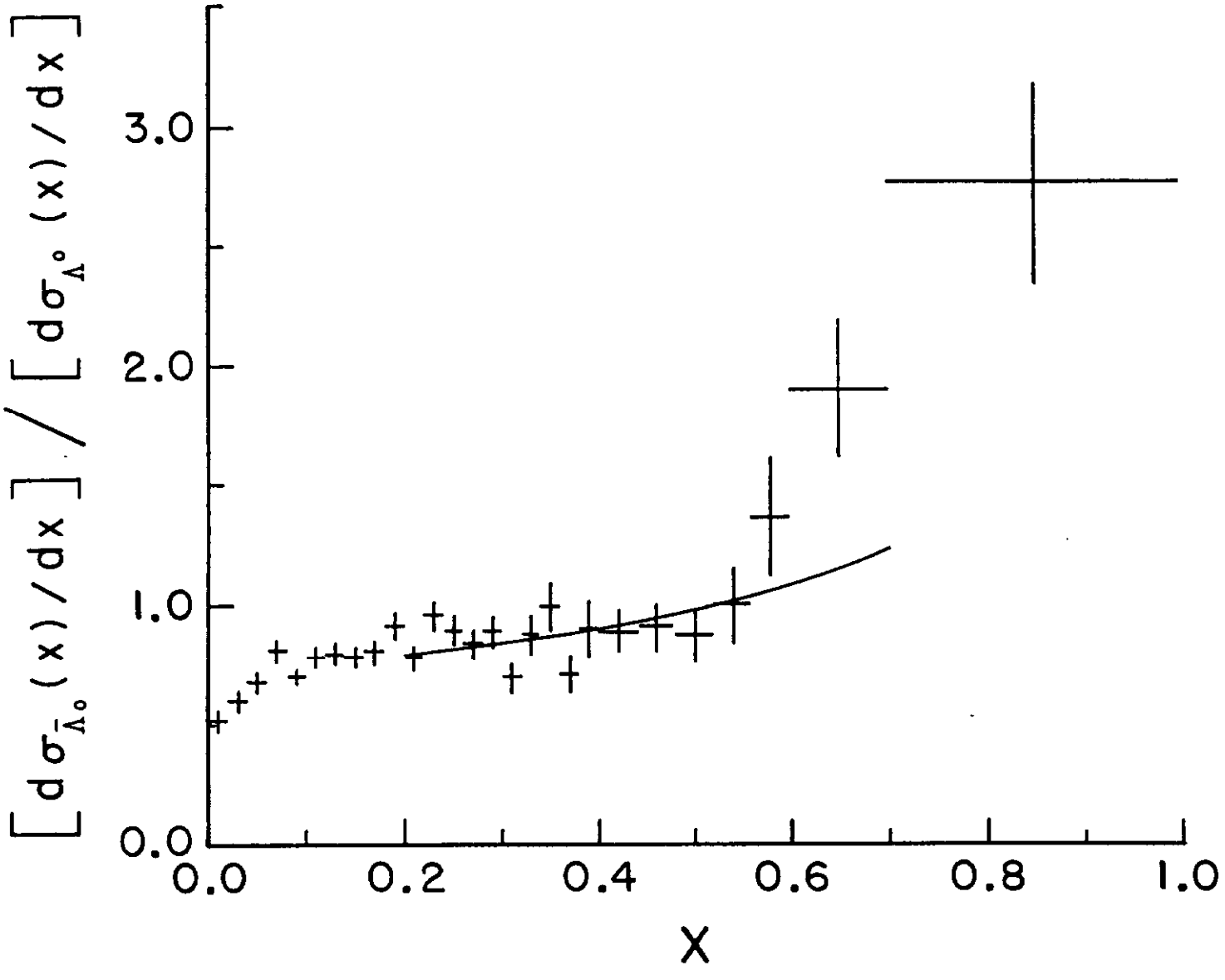

Figure 6

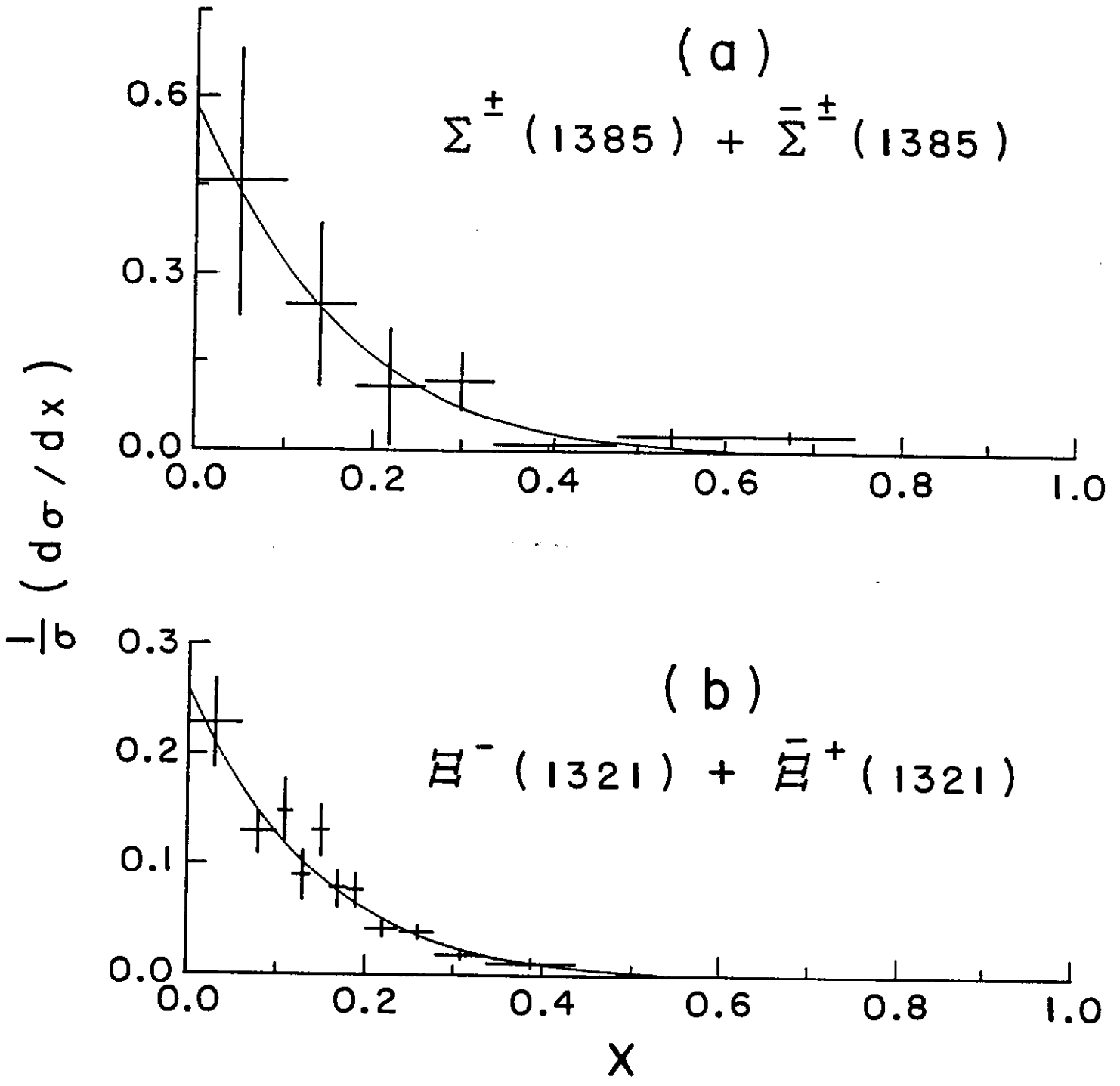
(a)
$\Sigma^{\pm}(1385) + \bar{\Sigma}^{\pm}(1385)$
(b)
$\Xi^{-}(1321) + \bar{\Xi}^{+}(1321)$
$\frac{1}{\sigma}\left(\frac{d\sigma}{dx}\right)$
X
0.0
0.2
0.4
0.6
0.8
1.0
0.1
0.3

Figure 7